![The University of Edinburgh logo]

THE UNIVERSITY *of* EDINBURGH

Edinburgh Research Explorer

Performance analysis of indoor diffuse VLC MIMO channels using Angular Diversity Detectors

OPEN ACCESS

Performance analysis of indoor diffuse VLC MIMO channels using Angular Diversity Detectors

Paul Fahamuel, *Student Member , IEEE,* John Thompson, *Member, IEEE,* and Harald Haas, *Member, IEEE*

Abstract—We consider specular and diffuse reflection models for indoor visible light communications (VLC) using a mobile receiver with angular diversity detectors in multiple input multiple output (MIMO) channels. We aim to improve the MIMO throughput compared to vertically oriented detectors by exploiting multipath reflections from different surfaces in the room. We then evaluate data throughput across multiple locations in the small room by using repetition coding, spatial multiplexing and spatial modulation approaches. In spatial modulation, we also propose a novel approach called adaptive spatial modulation (ASM). This makes use of channel matrix rank information to decide which TX/RX setup to be used, and is developed to cope with rank deficient channels. In a scenario where the receiver is moving, channel gains are weak in some locations due to the lack of line of sight (LOS) propagation between transmitters and receivers. This effect is mitigated by employing adaptive modulation and coding (AMC) together with per antenna rate control (PARC). We then compare the throughput for LOS only channels against LOS with specular or diffuse reflection conditions, for both vertical and angular oriented receivers. The results show that exploiting specular and diffuse reflections provide significant improvements in link performance.

P. Fahamuel is with the Dar es salaam Institute of Technology (DIT), Department of Electronics and Telecommunications Engineering, Tanzania. P. o Box 2958, Dar es salaam and with the University of Edinburgh, Institute for Digital Communications, the Kings Buildings, Edinburgh EH9 3JL, UK (e-mail: p.mmbaga@ed.ac.uk, pfahamuel@dit.ac.tz).

J. Thompson and H. Haas are with the University of Edinburgh, Institute for Digital Communications, the Kings Buildings, Edinburgh EH9 3JL, UK (e-mails:{john.thompson, h.haas}@ed.ac.uk)

I. INTRODUCTION

WITH the development of wireless communications applications, there is a rapid rise in data demand, while the available radio frequency (RF) spectrum cannot meet this growth and hence becomes the limiting factor for achieving higher transmission rates [1]. The spectrum ranging from $10\mu m$ (infra-red) to 10nm (ultraviolet) including visible light offers nearly limitless bandwidth which may be utilized for communications such as wireless local area networks (WLAN). In optical wireless communications, the light emitting diode transmitter modulates data and transforms the electrical signal to an optical signal while the photo-diode receiver converts the incoming optical signal into an electrical current for data processing. Optical wireless communications (OWC) therefore promises to be a low cost and high throughput alternative to RF communications. With the development of solid-state lighting, white light emitting diodes (LEDs) will replace existing conventional light bulbs so communications and illumination can take place simultaneously, hence saving power [2]. It is also safe to use in places where RF signals are not permitted e.g. hospitals, chemical plants and gas/petrol filling stations. Visible light communications is cheap because of the low cost and reliability of light sources and receivers.

Indoor OWC systems can be classified into diffuse and line of sight (LOS) systems. In LOS systems high data rates of the order of gigabits per second can be achieved [1], [3] but these systems are vulnerable to obstacles (shadowing) because of their directionality. In diffuse systems, several propagations paths exist from the LED to photo-diode (PD)

which makes the system robust to shadowing [4], however the path loss can be higher than for LOS systems and multipath creates inter-symbol interference (ISI) for the case of large area indoor environments [2], [5], [6]. The simultaneous use of multiple transmitters and receivers e.g. OWC multiple input multiple output (MIMO) can enhance the overall system performance and spectral efficiency as well as reducing the bit error ratio (BER) performance of a communication system [2]. MIMO systems can realize higher speed transmission without increasing the transmit power or the bandwidth.

Kahn and Barry gives more details about wireless infrared communication in [10]. Here the use of infrared radiation as a medium for high-speed, short range OWC is discussed, advantages and drawbacks are compared. MIMO techniques have been applied for OWC and data transmission to a limited extent. High data rate MIMO optical wireless communications using white LEDs were proposed in [2], where a fixed receiver with an imaging lens was used. It was shown that the imaging lens and detector array size are physically large and may not be practical for some applications. Another indoor OWC MIMO system with an imaging receiver was proposed in [7], here the diffuse environment experiments were performed. The system shows error-free operation at 2 Mbit/s/spatial channel at the center of the coverage area, with worse performance away from the center. In [8] results from several indoor OWC MIMO experiments were reported, a four channel MIMO system that uses white LEDs for communications was described as well as experiments in a diffuse environment using infra-red sources. An omnidirectional multibeam transmitter in [9] was proposed to improve transmission coverage and overcome shadowing, in this paper a multibeam hemispherical receiver structure was found to reduce multipath effects. The simulation results showed significant reduction of the BER making the system suitable for high bit rate applications.

Research development on overcoming channel correlation and inter-symbol interference yielded the method proposed in [11], [12]. Here indoor OWC MIMO using spatial modulation (SM) was sug-

gested and implemented, where unlike other MIMO techniques, only one transmitter is active at any given time instant. The active transmitter radiates at a certain intensity level and all other transmitters are turned off. In SM, it was found that reducing both the distance between transmitters (TX) and receivers (RX) and the transmitter emerging angle (the angle between TX axis and the straight line to the RX) resulted in lower correlation and hence higher data throughput. A hemispherical lens based imaging receiver for OWC MIMO was described in [13]. These papers presented a novel imaging MIMO optical wireless system which uses a hemispherical lens in the receiver, this system has both a wide field of view (FOV) and showed significant spatial diversity. In [14], a performance comparison of OWC MIMO Techniques in indoor environments was provided between repetition coding (RC), SM and spatial multiplexing. The results show that spatial multiplexing (SMP) improves the spectral efficiency when there is low channel correlation. It was also shown that SM is competitive at low spectral efficiency while SMP performs better in high spectral efficiency where SM needs a very large signal constellation size to match SMP. Also it is more robust to channel correlation. RC was found to be insensitive to different transmitter-receiver alignments but it needs a large signal constellation size to provide high data rates.

Wang and Armstrong in [15] analysed the performance of an indoor MIMO optical wireless system with a linear receiver. The receiver used an array of prisms to form channel matrices that can achieve angular diversity within a compact receiver structure. It was shown that full column rank can be achieved by the proposed receiver over an entire room. In [16] Wang and Chi experimentally demonstrated a 2×2 non-imaging MIMO VLC system that is capable to deliver 500Mb/s. However it was concluded that the large size of the lens and the detectors required are not practical. In [17], the receiver with angular diversity detectors was proposed and found to overcome the channel rank deficiency which occurs in areas away from the center of the room.

In these papers, the VLC coverage is among the

major drawbacks. In most papers movement of the receiver to different locations to asses the impact on channel correlation and hence spectral efficiency was not covered. Further the effect of diffuse channel reflections on MIMO was not discussed. The present paper addresses these issues and contains the following novel contributions:

- Propose a novel adaptive apatial modulation(ASM) method to tackle reduced channel rank.
- First evaluation of whole room MIMO performance using vertical and angular diversity receivers.
- Novel study of the impact of specular and diffuse reflections on MIMO performance.

We use a MIMO system taking into account line of sight (LOS) propagation, The Lambertian specular reflections model and the Lambert-Phong diffuse reflection model [4] for both vertical and angular oriented receiver detectors. We then provide performance statistics for MIMO methods operating over many room locations using adaptive modulation and coding (AMC), ASM, and per antenna rate control (PARC) [18]. We also consider RX performance improvement by application of angular diversity techniques.

The rest of the paper will be as follows. Section II presents the system models. Section III explains the MIMO techniques used in this paper. Section IV describes the evaluation of the system throughput. Section V shows the simulation parameters and the different simulation scenarios, along with the results and discussion. Section VI concludes the paper.

II. SYSTEM MODELS

We consider visible light communications (VLC) MIMO transmission and take into account both specular and diffuse reflections where intensity modulation (IM) and direct detection (DD) of the optical carrier using an incoherent light source is employed. The system consists of N_t transmitters and N_r photo-detectors at the receiver side. The size N_r received signal vector $\mathbf{y}$ is

$$\mathbf{y} = \mathbf{H}\mathbf{s} + \mathbf{n} \tag{1}$$
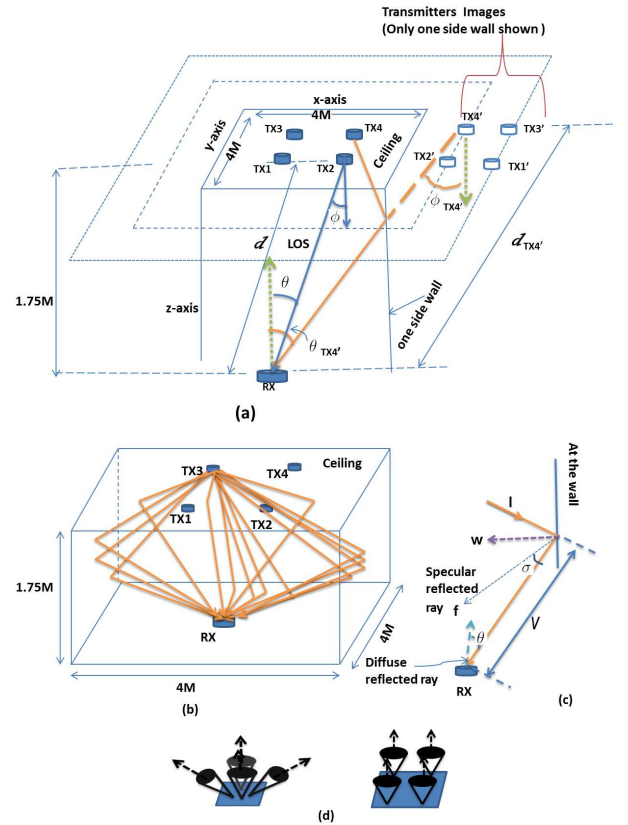
Fig. 1. Transmitter and receiver geometry used for channel coefficient calculations (a) Specular reflection model (b) Diffuse reflection model (c) Diffuse reflection-wall geometry (d) Receiver with inclined and vertical axis detectors

Where $\mathbf{H}$ is the $N_r \times N_t$ channel matrix and $\mathbf{s}$ is the transmitted signal vector which is transmitted at a given time and is defined as follows: $\mathbf{s} = [s_1 ......s_{Nt}]^T$ with $[.]^T$ being the transpose operator and s_n denoting the signal transmitted by n^{th} LED. The sum of the ambient light shot noise and thermal noise is denoted by $N_r \times 1$ vector $\mathbf{n}$ which is assumed to be real valued additive white Gaussian noise (AWGN) with zero mean and variance:

$$\delta^2 = \delta^2_{\text{shot}} + \delta^2_{\text{thermal}} \tag{2}$$

Where δ^2_{shot} is the shot noise variance and $\delta^2_{\text{thermal}}$ is the thermal noise variance as calculated in equations (7) and (10) of [6] respectively. Thus the noise power is given by $\delta^2 = N_0 B$, where N_0 is the noise power spectral density and B is communication bandwidth.

This paper assumes an optical wireless LOS link operating in a room with reflection characteristics

(Fig. 1). There are two types of reflections considered in this paper. The first type is a single bounce specular reflection which is modelled by an image transmitter TX'_n to the receiver (Fig. 1. a). The reflections cause the signal to be attenuated by the surface reflection coefficient α. The second type is a single bounce diffuse reflection where all the rays bouncing from the reflecting surface is scattered into different directions of the room (Fig. 1. b). The incidence power from the wall is assumed to be a fraction of the total transmitted power wich is dictated by the number of rays re-radiated.

The LOS $N_r \times N_t$ channel matrix $\mathbf{H}$ for each room coordinate (x, y, z) in the room is given by

$$\mathbf{H}(x,y,z)_{LOS} = \begin{pmatrix} h_{11}(x,y,z) & h_{12}(x,y,z) & . & . & h_{1N_t}(x,y,z) \\ h_{21}(x,y,z) & h_{22}(x,y,z) & & & . \\ . & & . & & . \\ . & & & . & . \\ h_{Nr1}(x,y,z) & & . & . & h_{NrNt}(x,y,z) \end{pmatrix} \tag{3}$$

where $h_{n_r n_t}$ represents the channel transfer function of the wireless link between transmitter n_t and receiver n_r. For the specular reflection model (S_p) (Fig. 1 (a)) and the diffuse reflection model (D_f) (Fig. 1 (b)), the total channel gain at the receiver detector n_r from transmitter n_t is

$$h_{n_r n_{t(S_p/D_f)}} = \sum_{i=1}^{N_{TXn}} h_{n_r n_{ti}} \tag{4}$$

where for S_p, N_{TXn} is the number of transmitter images received at detector n_r caused by transmitter n_t and for D_f N_{TXn} is the number of scattered light rays received from transmitter n_t. Therefore, Therefore, when all LOS rays and SR or DR rays are considered with only first bounce, the channel gain at the individual receiver detector n_r will be

$$h_{n_r n_{t(\text{Total})}} = h_{n_r n_{t(LOS)}} + h_{n_r n_{t(S_p/D_f)}} \tag{5}$$

So, the overall $N_r \times N_t$ channel matrix $\mathbf{H}$ for each room coordinate (x, y, z) in the room will be represented by substituting (5) into (3). The path difference between the multiple transmitter-receiver links is very small, on the order of few cm as shown in Fig. 1. We assume for simplicity that the communications channel bandwidth is much less

than the inverse of the delay spread, so the channel is not frequency selective.

By using the Lambert-Phong method [4] the diffuse paths are assumed to be scattered paths re-radiated from the wall to the receiver after being attenuated by the surface reflection coefficient α. As illustrated in Fig. 1 (a), $\phi_{TX'_n}$ is the angle of emergence with respect to the image of transmitter TX_n axis, θ_{TXn} is the angle of incidence with respect to the receiver detector axis and $d_{TX'_n}$ is the distance between the image transmitter TX'_n and receiver. Also as illustrated in Fig. 1 (c), σ is the angle of emergence with respect to the direction of specular reflected ray axis $\mathbf{f}$ which is a directional vector with coordinates (x, y, z), θ is the angle of incidence with respect to the receiver detector axis and V is the distance between the reflecting point and the receiver. The system transmitters are fixed at the following ceiling coordinates:
TX_1[1.9 m, 1.9 m, 2.75 m], TX_2[2.5 m, 1.9 m, 2.75 m], TX_3[1.9 m, 2.5 m, 2.75 m], and TX_4[2.5 m, 2.5 m, 2.75 m].

The transmitters are arranged in a square in the middle of the ceiling and the antenna side separation is 0.6m as this choice was found to reduce channel correlation in [17].

Consider a LOS optical system propagation path in Fig. 1, the channel gain from the transmitter to the receiver is given by [14]:

$$h = \begin{cases} \frac{A(k+1)\cos^k(\phi)\cos(\theta)}{2\pi d^2}, & 0 \leqslant \theta \leqslant \varphi_{1/2} \\ \\ 0, & \theta > \varphi_{1/2} \end{cases} \tag{6}$$

where $k = \frac{-\ln(2)}{\ln(\cos(\Phi_{1/2}))}$.

The scalar A is the collection area of the receiver n_r, $\Phi_{1/2}$ is the transmitter semi-angle (at half power), which is assumed to be 45°. The scalar $\varphi_{1/2}$ is the Field of View (FOV) semi angle of the receiver which is also assumed to be 45°. In [14] $\Phi_{1/2}$ and $\varphi_{1/2}$ were assumed to be both 15°, but for this setup where the receiver is moving around the room, it is difficult to achieve LOS channel conditions in many locations when a narrower half angle is used. We set $h_{n_r n_{t(LOS)}} = 0$, when a transmitter is not in the FOV of the receiver. Image transmitters in the specular

reflection model use the same equation (6) with their respective angles, then the gain is multiplied by the reflection attenuation α to yield the corresponding channel coefficient

$$h = \alpha \frac{A(k+1)}{2\pi d_{TX_n}^{'2}} \cos^k(\phi_{TX_n}^{'}) \cos(\theta_{TX_n}^{'}) \qquad (7)$$

For the diffuse reflection case the Lambert-Phong model is used [4]. We define a reflection intensity scattering using a generalized Lambert radiation pattern

$$P_{Wall} = \alpha \frac{P_i(m_s+1)}{2\pi} \cos^{m_s}(\sigma) \qquad (8)$$

where P_i is the incident normalized unit power arriving at the wall, P_{Wall} is the reflection intensity from the reflecting surface, m_s is the smoothness of the reflecting material and σ is the randomly generated parameter which represents the angle between specular reflected rays and the diffuse reflected ray (Fig. 1. c). To calculate the specular reflected ray vector $\mathbf{f}$ we make use of the normal vector $\mathbf{n}$ to the wall and the vector $\mathbf{l}$ which is the line connecting transmitter and the wall (see Fig. 1. c):

$$\mathbf{f} = (2\mathbf{w} \bullet \mathbf{l})\mathbf{w} - \mathbf{l} \qquad (9)$$

where $\mathbf{f}$, $\mathbf{w}$ and $\mathbf{l}$ are three dimensional vectors with components (x, y, z). The dot mark in (9) denotes the vector dot product. As shown in Fig. 1. c, once $\mathbf{f}$ and σ are known then all the diffusely reflected paths can be generated. So, the channel gain for one reflected ray from the wall to the receiver is expressed as

$$h(\sigma, m_s) = \begin{cases} \alpha \frac{A(m_s+1)}{2\pi V^2} \cos^{m_s}(\sigma)\cos(\theta), & 0 \leqslant \theta \leqslant \varphi_{1/2} \\ \\ 0, & \theta > \varphi_{1/2} \end{cases} \qquad (10)$$

and the incident optical power to the receiver, see [6], [19] can be calculated by

$$P_{ir} = P_{Wall} \frac{A\cos(\theta)}{V^2} = h(\sigma, m_s)P_i \qquad (11)$$

We now briefly describe the technique used for configuring the inclined optical detectors of the receiver. The left side of Fig.1(d) shows the receiver with inclined detectors. To achieve this setup the detector axis vector $\mathbf{z}$ which is inclined at an elevation angle 45° is transformed around the z axis (vertical axis) using the transformation matrix as in [17]. The orientation angle of the receiver in the $x - y$ plane is assumed to be random, which is likely to be the case in practice as different users will hold their devices in different orientations. The orientation of the receiver is given by

$$\hat{\mathbf{z}} \quad = \quad \mathbf{R_z}(\vartheta + \omega) \quad \times \mathbf{z}$$

$$\begin{pmatrix} \hat{x} \\ \hat{y} \\ \hat{z} \end{pmatrix} = \begin{pmatrix} \cos(\vartheta+\omega) & -\sin(\vartheta+\omega) & 0 \\ \sin(\vartheta+\omega) & \cos(\vartheta+\omega) & 0 \\ 0 & 0 & 1 \end{pmatrix} \begin{pmatrix} x \\ y \\ z \end{pmatrix} \qquad (12)$$

where $\hat{\mathbf{z}}$ is the transformed vector, ϑ presents the transformation angle around the z axis to form the detectors' axis vectors pointing at azimuth angles 0°, 90° 180° and 270° with an additional random rotation angle ω which is uniformly distributed between 0° to 360°. The matrix $\mathbf{R_z}$ is the transformation matrix with respect to the z axis.
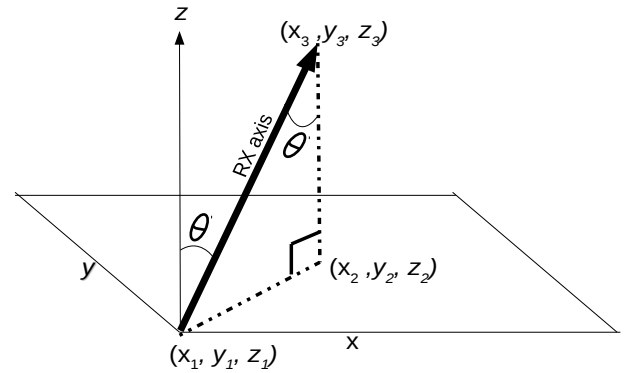
Fig. 2. Geometry for elevation angle calculations

Since any variation of the detector's axis affects the angle of incidence θ as in (6) and (10), each detector elevation angle is varied from 45° to 90° (0° from vertical)(see Fig. 2) to find the elevation angle that will maximize the rank of channel matrix $\mathbf{H}$. Therefore a single selected elevation angle is used for the inclined axis detector for system

performance evaluation at all locations in the room. From Figure 2 the angle of elevation of the inclined receiver can be given by:

$$\theta = \sin^{-1}\left(\sqrt{\frac{(x_1 - x_2)^2 + (y_1 - y_2)^2 + (z_1 - z_2)^2}{(x_1 - x_3)^2 + (y_1 - y_3)^2 + (z_1 - z_3)^2}}\right) \tag{13}$$

where, (x, y, z) are the coordinates in three dimension

III. MIMO TECHNIQUES

In this paper four different MIMO techniques are used; repetition coding (RC) for improving Diversity gain, spatial modulation (SM) for improving energy efficiency, adaptive spatial modulation (ASM) also for improving energy efficiency and spatial multiplexing (SMP) for improving multiplexing gain as in [17]. In contrast to [2], [8], [11] where fixed receivers are used, in this paper we consider that mobile receiver is able to move freely around the room as in [17]. To overcome the resulting SNR variations we employ adaptive modulation with per antenna rate control (PARC) [18] in SMP and adaptive modulation in SM and RC. In these techniques, the modulation M-level is chosen and updated in each transmit time and at each location depending on the current channel conditions. We assume that all considered MIMO techniques use maximum likelihood (ML) [14] detection at the receiver with perfect knowledge of the channel and ideal time synchronisation except in SMP where the zero forcing (ZF) detection method is used to reduce receiver complexity when using PARC. Therefore in RC, SM and ASM the decoder selects a constellation vector $\hat{\mathbf{s}}$ which minimizes the Euclidean distance between the actual received signal $\mathbf{y}$ and all the possible signal vectors leading to

$$\hat{\mathbf{s}} = \arg\max_{\mathbf{s}} p_{\mathbf{y}}(\mathbf{y}|\mathbf{s}, \mathbf{H}) = \underset{\mathbf{s}}{\text{argmin}} ||\mathbf{y} - \mathbf{Hs}||_F^2 \tag{14}$$

where $p_{\mathbf{y}}$ is the probability density function of $\mathbf{y}$ conditioned on s and $\mathbf{H}$. The notation $||.||_F$ indicates the Frobenius norm.

A. Repetition coding (RC)

The first technique used is RC which simultaneously emits the same signal from all transmitters. Therefore the condition $s_1 = s_2 = ...s_{Nt}$ holds [14]. In RC, the light intensities arising from the several transmitters constructively add up at the receiver side. In this paper, unipolar M-level pulse amplitude modulation (M-PAM) is considered together with RC, where M denotes the signal constellation size. Therefore M-PAM achieves a spectral efficiency of $\log_2(M)$bit/s/Hz. PAM is more bandwidth efficient compared to other pulse modulation techniques such as pulse-width modulation (PWM), on-off keying (OOK) and pulse -position modulation (PPM). [14]. Moreover PAM has been shown to outperform direct current biased optical OFDM (DCO-OFDM) because the later requires a high constant DC bias to make the bipolar OFDM waveform non-negative [14]. We employ rectangular pulse shapes with M-PAM, so the intensity level emitted by the Light Emitting Diode (LED) is given by

$$I_m^{PAM} = \frac{2I}{M-1}m, \text{ for } m = 0, 1, ...(M-1) \tag{15}$$

where I is the mean optical power emitted. The Bit Error Rate (BER) for unipolar M-PAM can be expressed by

$$\text{BER}_{\text{PAM}} \leqslant \frac{2(M-1)}{M\log_2(M)}Q\left(\frac{1}{M-1}\sqrt{\frac{E_{RX}}{N_0}}\right) \tag{16}$$

where:

$$Q(a) = \frac{1}{\sqrt{2\pi}}\int_a^{+\infty}\exp\left(\frac{-t^2}{2}\right)dt \tag{17}$$

is the Q function [14] and E_{RX} is the received electrical energy. The BER of M-PAM given in (16) can be generalized for the $N_r \times N_t$ scenario and the resulting BER is given by:

$$\text{BER}_{\text{RC}} \leq \frac{2(M-1)}{M\log_2(M)}Q\left(\frac{1}{M-1}\sqrt{\frac{E_s}{N_0 N_t^2}\sum_{n_r=1}^{N_r}\left(\sum_{n_t=1}^{N_t}h_{n_r n_t}\right)^2}\right) \tag{18}$$

Where, $E_s = (\varrho I)^2 T_s$ denotes the mean emitted electrical energy of the intensity modulated optical signals. The symbol ϱ represents the optical to

electrical conversion coefficient, it is assumed that, $\varrho = 1\Lambda/\text{W}$. The scalar T_s denotes the symbol duration in seconds and Λ is the unit current in amperes.

B. Spatial Modulation (SM)

The second technique used in this paper is SM, which combines MIMO and digital modulation as proposed in [20] and further investigated in [21], [28], [30] and also applied in [12]. In SM the conventional constellation diagram is extended to an additional dimension namely, the spatial dimension. Specifically, the LED index is used to communicate data bits to the receiver. Each transmitting LED is assigned a unique binary sequence (the spatial symbol). A transmitter is only activated when the
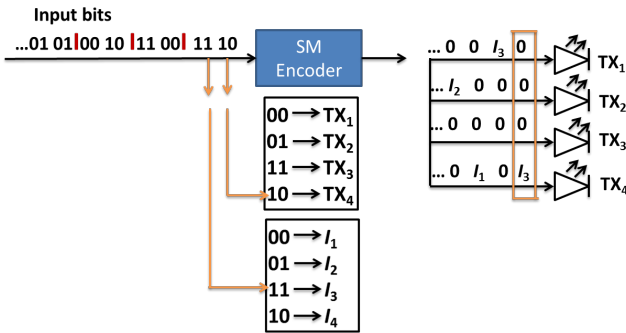

Fig. 3. Illustration of SM operation with $N_t = 4$ and $M = 4$. The first two bits in the block of four bits determine the PAM symbol and second two bits determine the active LED [12]

random spatial symbol to be transmitted matches the specified transmitter index. Thus, only one transmitter is activated for any PAM symbol transmission so only one element of the signal vector **s** to be transmitted is non-zero. SM can provide an enhanced spectral efficiency of $\log_2(N_t) + \log_2(M)$ bit/s/Hz, see in [11], [12], [19], [20], [24]–[27]. Signals with intensity $I_m = 0$ cannot be used for the signal modulation of SM, because in this case no transmitter would be active and the spatial information information would be lost [14], [29]. Therefore, the intensities of conventional PAM given in (7) have to be modified to be compatible with SM leading to:

$$I_m^{\text{SM}} = \frac{2I}{M+1}m, \ \text{for} \ m = 1, ...(M) \quad (19)$$

The BER expression for SM is given by:

$$\text{BER}_{\text{SM}} \leq \frac{1}{MN_t \log_2(MN_t)} \sum_{m^{(1)}=1}^{M} \sum_{n_t^{(1)}=1}^{N_t} \sum_{m^{(2)}=1}^{M} \sum_{n_t^{(2)}=1}^{N_t} d_{\text{H}}\left(b_{m^{(1)}n_t^{(1)}}, b_{m^{(2)}n_t^{(2)}}\right)$$
$$Q\left(\sqrt{\frac{E_s}{4 N_0} \sum_{n_r=1}^{N_r} \mid I_{m^{(2)}}^{\text{SM}} h_{n_r n_t^{(2)}} - I_{m^{(1)}}^{\text{SM}} h_{n_r n_t^{(1)}} \mid^2}\right) \quad (20)$$

Where, $d_{\text{H}}\left(b_{m^{(1)}}, b_{m^{(2)}}\right)$ denotes the Hamming distance of two bit assignments $b_{m^{(1)}}$ and $b_{m^{(2)}}$ of the signal vectors $\mathbf{s}_{m^{(1)}}$ at the transmitter and signal $\mathbf{s}_{m^{(2)}}$ at the receiver.

C. Adaptive Spatial Modulation (ASM)

The third technique is ASM which is a modified form of spatial modulation (SM). ASM is proposed in this paper to cope with rank deficient channels due to the fact that, when the receiver moves around the room the channel matrix **H** is not full rank (4) in many locations. If the channel matrix rank is reduced, the receiver can not easily distinguish all the transmitting LEDs. By using antenna selection techniques, the ASM receiver checks the rank of the channel matrix and decides which TX/RX setup to be used.

The authors in [22], [23], [25] proposed some different techniques for antenna selection. This paper will discus the methods proposed in [25] which is relevant to the technique proposed in this paper. In [25] they use two methods which reduce the order of complexity (number of times the optimization metric is evaluated). The first method was a Euclidean distance optimized antenna selection (EDAS) which chooses the specific antenna set that maximizes the minimum Euclidean distance among all the possible transmit vectors. The second one was capacity optimized antenna selection (COAS) which uses the bounded system capacity to chooses the set of antennas corresponding to the largest channel norms out of number of transmitting antennas. In this paper a similar method to COAS is used but with the difference that the system capacity is not used as the metric as it is not applicable to positive real channels that arise in OWC. Instead the channel matrix rank is used here to decide the number of antennas to be active, thereafter the largest channel norms will be

used to decide the set of antennas to be used. The following three steps are involved.

- If rank(**H**)=4, we use four transmitter Adaptive Modulation SM for transmission and throughput calculations.
- If rank(**H**)=2 or 3, we employ 2TX Adaptive Modulation SM. To identify which two transmitters are to be activated we check the **H** matrix using the norm based method (22). Assume $\mathbf{q_{n_t}}$ is the column of **H** as follows:

$$
\mathbf{q_{n_t}} = \begin{pmatrix} h_{1\ n_t} \\ . \\ . \\ . \\ . \\ h_{Nr\ n_t} \end{pmatrix}, \quad n_t = 1, ..., N_t \quad (21)
$$

Then we select the two highest norm of sum of each $\mathbf{q_{n_t}}$ values such that the selected two norms will present the column of transmitters TX_1 and TX_2:

$$
\text{Norm}_{n_t} = \sum_{n_r=1}^{N_r} \mid h_{n_r n_t} \mid , \ n_t = 1.....N_t. \quad (22)
$$

then we sort the norms in decreasing order so that the first two largest norms identify transmitters to be selected.

- If rank(**H**)=1, we use RC with Adaptive Modulation.

If Ω denotes the number of selected antennas, the BER of ASM is approximated using the joint BER evaluation method. This uses both the SM and the RC BERs as used in [14], which are jointly evaluated as follows :

$$
\text{BER}_{\text{ASM}} \leq \begin{cases} \frac{1}{M\Omega}\frac{1}{\log_2(M\Omega)} \sum_{m^{(1)}=1}^{M} \sum_{n_t^{(1)}=1}^{\Omega} \sum_{m^{(2)}=1}^{M} \sum_{n_t^{(2)}=1}^{\Omega} d_{\text{H}}\left(b_{m^{(1)}n_t^{(1)}}, b_{m^{(2)}n_t^{(2)}} \right) \cdot \\ Q\left(\sqrt{\frac{g^2 T_s}{4 N_0} \sum_{n_r=1}^{N_r} \mid I_{m^{(2)}}^{\text{SM}} h'_{n_r n_t^{(2)}} - I_{m^{(1)}}^{\text{SM}} h'_{n_r n_t^{(1)}} \mid^2} \right), \qquad 2 \leq \Omega \leq 4 \\ \frac{2(M-1)}{M \log_2(M)} Q\left(\frac{1}{M-1} \sqrt{\frac{E_s}{N_0 N_t^2} \sum_{n_r=1}^{N_r} \left(\sum_{n_t=1}^{N_t} h_{n_r n_t} \right)^2} \right), \qquad \Omega = 1 \end{cases} \quad (23)
$$

In this equation $h'_{n_r n_t}$ denotes the channel coefficients of the selected antennas.

D. Spatial Multiplexing (SMP)

The final MIMO technique is SMP. In SMP independent data streams are simultaneously transmitted from all the transmitters. Since ZF is used to estimate the transmitted symbol in SMP, the following equation is used to obtain the estimate value of **s**: Consider equation (1),

$$
\hat{\mathbf{s}} = \mathbf{W} \cdot \mathbf{y} \quad (24)
$$

where, **W** denotes the Pseudo-inverse of channel matrix **H** which is given by:

$$
\mathbf{W} = (\mathbf{H}^T \mathbf{H})^{-1} \mathbf{H}^T \quad (25)
$$

SMP provides a maximum spectral efficiency of $N_t \log_2(M)$ bit/s/Hz. As for RC, PAM is used with SMP and equally distributes the optical power across all emitters to ensure that both schemes use the same transmit power. The BER for SMP is given as:

$$
\text{BER}_{\text{SMP}} \leq \frac{1}{N_t} \sum_{i=1}^{N_t} \frac{2(M_i - 1)}{M_i \log_2(M_i)} Q\left(\frac{1}{M_i - 1} \sqrt{\frac{E_s}{N_0 N_t^2 \parallel \mathbf{W}_i \parallel^2}} \right) \quad (26)
$$

where, $\mathbf{W}_i$ denotes i^{th} row of pseudo-inverse of channel matrix **H**, M_i is the ith selected modulation level for transmitter LED i.

IV. SYSTEM THROUGHPUT EVALUATION

For the RC techniques we use the BER Expression described in equation (18) and calculate throughput given by [6]:

$$
T_{h(\text{SISO})} = R(1 - \gamma) \text{ bps/Hz} \quad (27)
$$

Where R is the maximum rate of the scheme and γ is the packet error probability which is given by [6]:

$$
\gamma = 1 - (1 - BER)^{N_b} \quad (28)
$$

Where, N_b is the number of bits in one packet. Equation (27) is computed for all modulation sizes M which yield a BER less than 10^{-2} (see Fig. 3 of [17]). Then, the highest throughput determines the modulation scheme that is selected. A BER greater values than 10^{-2} is ignored since will not give a substantial throughput gain as shown in Fig. 3. of [17].

For SM, the BER calculations is carried out using equations 20 and the technique for selecting the best BER is the same as in RC. The verall throughput is calculated using the following equation:

$$T_{h(\text{MIMO})}(x, y, z) = Th_{\text{BER}_{Mi}} \qquad (29)$$

For ASM, after the process explained in sub-section (c) of (III) has been performed, the BER calculations is carried out based on equation (23), and also choose the highest modulation level which gives the highest throughput such that the BER is less than 10^{-2}. The overall throughput is calculated using the following equation:

$$T_{h(\text{MIMO})}(x, y, z) = Th_{\text{BER}_{N_T Mi}} \qquad (30)$$

Where, N_T denotes number of selected transmitters (LEDs) in a given channel rank condition.

For SMP we use the similar approach as in RC except that, in this case we use Adaptive modulation with PARC [18] to optimize the choice of modulation separately for each transmitter. For each possible set of modulation schemes, we compute the BER expression as in equation (26) and choose the highest modulation level which gives the highest throughput such that the BER is less than 10^{-2}:

$$T_{h(\text{MIMO})}(x, y, z) = \sum_{i=1}^{N_T} Th_{\text{BER}_{\text{TX}iMi}} \qquad (31)$$

Where $Th_{\text{BER}_{\text{TX}iMi}}$ denotes throughput for an individual LED with an appropriate modulation while N_T presents the number of transmitting LEDs.

V. SIMULATION PARAMETERS AND RESULTS

We consider a 4×4 indoor MIMO scenario as in [17], but in this paper we also consider the effect of wall reflections. The system is located within a room of size $4 \times 4 \times 3$ m and we assume the transmitters are placed at a height of 2.50 m and oriented downwards perpendicular to the floor of the room. The receiver is allowed to move randomly at a height of 0.75 m (human waist or table height) and its detectors are either placed vertically or oriented at a given elevation angle as in Fig. 1 (d). The inclined detectors orientation is meant to increase the likelihood of a given transmitter being in the

TABLE I.   PARAMETERS USED FOR SIMULATION

Parameters	Values
Room size ($W \times L \times H$)	4 m ×4 m× 3 m
Number of TX/RX	4×4
TX separation	0.6 m
Reflection coefficients (α)	0.1, 0.3, 0.5, 0.7, 0.9 ([4], [9])
Reflection parameter (m_s)	1 (rough surface)
RX separations (V. detectors)	0.1 m
Photodiode responsivity (ϱ)	1 Λ/W
RX random rotation angles	0° to 360°
RX FOV	45°
RX elevation angle (A. Diversity)	45° to 90° towards vertical
RX azimuth angle separation (A. Diversity)	90°
Photodiode area (A)	1cm^2
MIMO transmission techniques	RC, SM, ASM, SMP
Modulation schemes	2PAM-1024PAM

FOV of one of the receivers and also incoming reflected rays to the receiver, thus increasing system spectral efficiency.

A computer program that implements the scenarios presented in previous sections was written using MATLAB software. The simulation parameters are tabulated in Table I. The room size shows the dimension of the room where the simulation is assumed. The TX/RX setup defines the number of transmitters and receivers used in simulation. The TX separation shows how far the four transmitting LEDs are separated from each other, the RX separation shows how the receiver detectors are separated (this applies for the vertically oriented receiver). The RX FOV is the field of view angle for the receiver. The RX detectors elevation angle is the one between detector's axis and the horizontal. For angular oriented detectors (A. detectors) this angle is varied to determine the optimum one while for the vertically oriented detectors (V. detectors) the angle of elevation is always 90° from the horizontal plane. The RX detectors azimuth angle separation shows how four detectors are angularly separated around 360° for the angular diversity detectors setup (A. detectors). We assume users hold their devices in a random orientation in the range of $0^o - 360^o$ azimuth angles from the position of the detector. This is achieved by applying (12) to all the detector locations. The experiment set-up and system performance comparison are presented in the next subsections:

A. Setting up Vertical detectors

To validate our results, the setup developed in [14] was repeated for all proposed MIMO transmission techniques and different TX separations (0.2 m, 0.4 m, 0.6 m). The RX detector separation remains 0.1m all the time with a vertically oriented RX as in Fig. 1(d) right. The BER results for a data rate of $R = 4$ bps/Hz are plotted as shown in Fig. 2 of [17]. These results match well with Fig. 3(a) of [14] and show the validity of the simulator.

We then developed a mobile receiver model and evaluated the throughput for 1000 locations. The location (x,y coordinates) are uniformly distributed and once the location and orientation parameters are defined, the channel matrix $\mathbf{H}$ is fixed. In this case (of a mobile receiver) we employ adaptive modulation for all transmission techniques, i.e. the rate of transmission is updated at each room location depending on the channel conditions. In addition to adaptive modulation we consider PARC in SMP. The results for average throughputs of the different transmission techniques and different reflection coefficients are compared in Table III and IV. Further, the CDF for all techniques are shown in Fig. 6, 7, 8 and 9. Both data tables and CDF plots are explained in subsection V-B.

B. Comparison between Vertical detectors and Angular diversity detectors with specular and diffuse reflections.

Here we compare the performance of vertical detectors and angular diversity detectors for a mobile receiver taking into consideration the effects of wall reflections and receiver. All the setups were simulated using all the MIMO transmission techniques discussed in section III. Using the throughput calculations in section IV, typical average throughput results for all setups (vertically oriented and angular diversity detectors) and their scenarios (reflection types and reflection coefficients) are tabulated in Table III and IV. Results are shown for four techniques (RC, SM, ASM and SMP), with both V. detectors (Vertically oriented detectors) and A. detectors (angular diversity detectors). Fig. 5. shows the SMP CDF comparison for three different elevation angles in angular diversity receiver (10º, 15º and 20º) when

LOS, LOS + Df and LOS + Sp are considered. Elevation angles. Looking at the A. detectors (LOS + Dif) results on the same figure we can see that elevation angles of 10º, 15º and 20º give throughputs of 24.8 bps/Hz, 29.2 bps/Hz and 22.3 bps/Hz respectively and therefore 15º is used in all the subsequent simulation results to allow a fixed receiver design which does not require mechanical tilting of the receiver sensors at different room locations. Fig. 6. shows the RC CDF comparison between V. detectors and A. detectors with and without reflections, also with different reflection coefficients. For simplicity only the CDF results for reflection coefficients of 0.3, 0.5, and 0.7 are plotted for all the curves, other results are recorded in Tables III and IV.

1) Results for the LOS channel:

Table II shows results for different antenna separations matching to Table II of [17] where the four techniques (RC, SM, ASM, SMP) in LOS were compared in detail. Looking at the table we can see that, for a moving angular diversity receiver there is an improvement in throughput when using SMP with PARC compared to other techniques (RC, SM and ASM). Percentage wise, for a TX separation of 0.4m, SMP performs 46% and 144% better than RC for V. Detectors and A. Detectors respectively. In comparison to ASM, SMP performs 41% and 120% better for V. Detectors and A. Detectors respectively.

TABLE II.   SIMULATION RESULTS FOR LOS WITH DIFFERENT ANTENNA SEPARATIONS

Trans-mission Method	Average throughput in bps/Hz					
	V. detectors (0º)			A. detectors (15º)		
	0.2 m	0.4 m	0.6 m	0.2 m	0.4 m	0.6 m
RC	5.2	5.6	6	6.5	6.3	6.4
SM	1.1	1.3	1.8	1.7	2.2	2.9
ASM	5.2	5.8	7.6	6.1	7	10.1
SMP	6	8.2	13.2	13	15.4	18.7

Legend:
V=Vertically oriented, A=Angular diversity
0.2 m to **0.6 m** are the transmitter separations

For a TX separation of 0.6m, SMP performs 120% and 192% better than RC for V. Detectors and A. Detectors respectively and when compared to ASM, SMP performs 78.9% and 85.1% better for V. Detectors and A. Detectors respectively. All the subsequent results in this paper are for 0.6m transmitter spacing as this spacing provides the best performance in Table II. Here, we also consider the channel rank of different receiver locations in
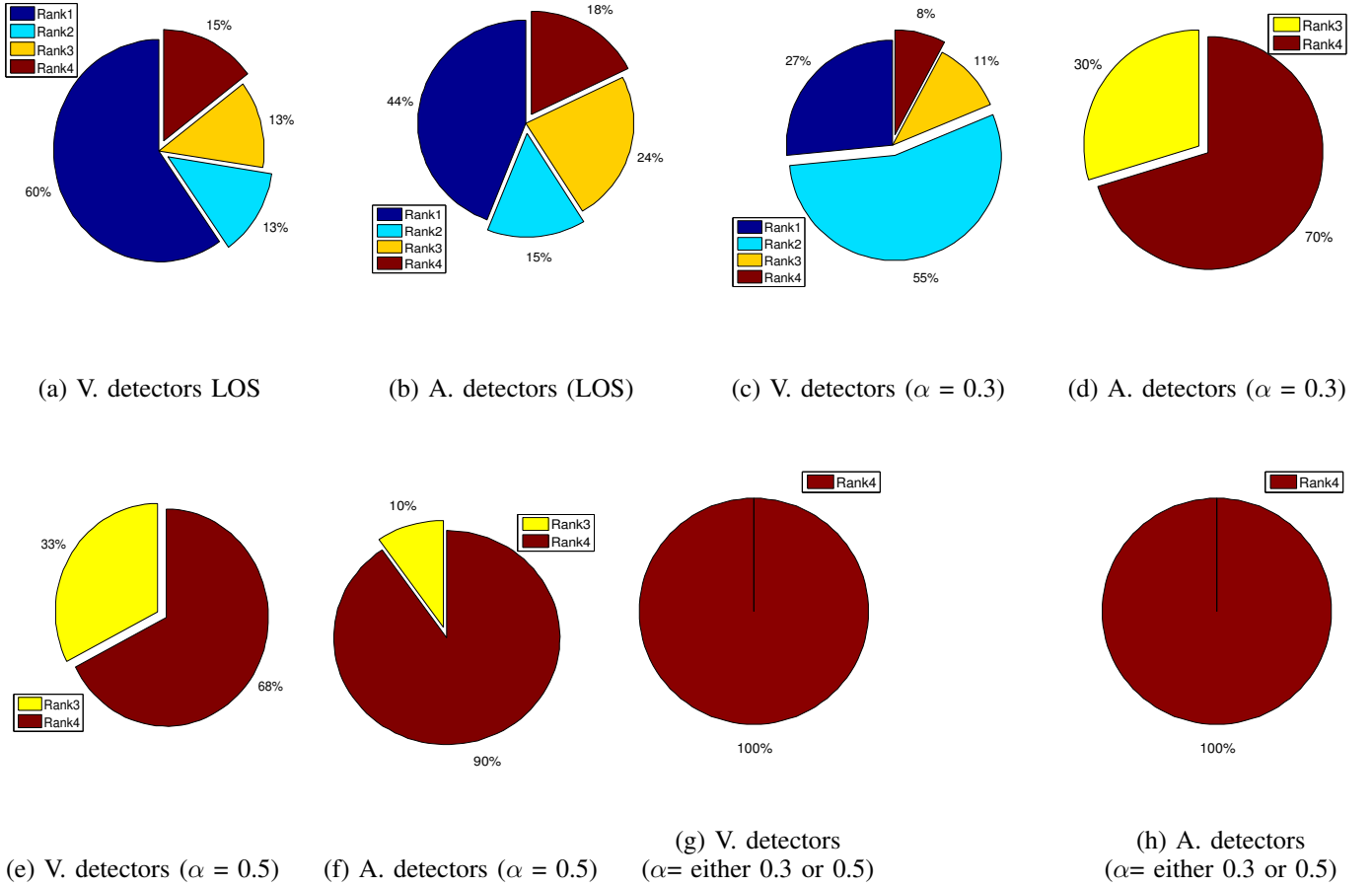
Fig. 4. Percentage distributions of MIMO channels matrix rank in 1000 locations of the room (a) Vertical detectors setup (b) Angular diversity detectors setup (c & e) Vertical detector setup with specular reflections (d &f) Angular diversity detectors setup with specular reflections (g & h) Both vertical and angular detectors setups with diffuse reflections

the room. Looking at Fig. 4(a) we can see that the channel matrix rank for the vertical detector is 1 for a large area of the room (60%) while in Fig. 4(b) the proportion is reduced for the angular diversity detectors (44%) which indicates a higher potential for MIMO receivers. We can see in Fig. 6. that the difference between the two setups in LOS conditions mainly relates to the coverage where 10% of the V. detectors setup give zero throughput to the total loss of LOS paths between TX and RX. The A. detectors setup gives non zero throughput results in all room locations.

2) Results for the LOS with specular reflection channel:

We can also see the effects of reflections when we look at Fig. 4(c) through (h). In Fig. 4(c) when

specular reflection with a reflection coefficient $\alpha = 0.3$ is considered in V. detectors, the proportion of rank 1 channels reduces to 27% and rank 2 increases to 55%. In Fig. 4(d) when specular reflections ($\alpha = 0.3$) are included in the A. detectors setup, the channel matrix rank values are either only 3 (30%) and 4 (70%) as the chance of multipath reception has increased. Also in Fig. 4(e) when specular reflections ($\alpha = 0.5$) are included in the V. detectors setup, the channel matrix rank is either 3 (33%) or 4 (68%) as the chance of multipath reception has further increased compared to V. detectors ($\alpha = 0.3$). Fig 4(f) shows the effect of specular reflections on A. detectors ($\alpha = 0.5$), the rank 4 case dominates (90%) and only 10% of channels
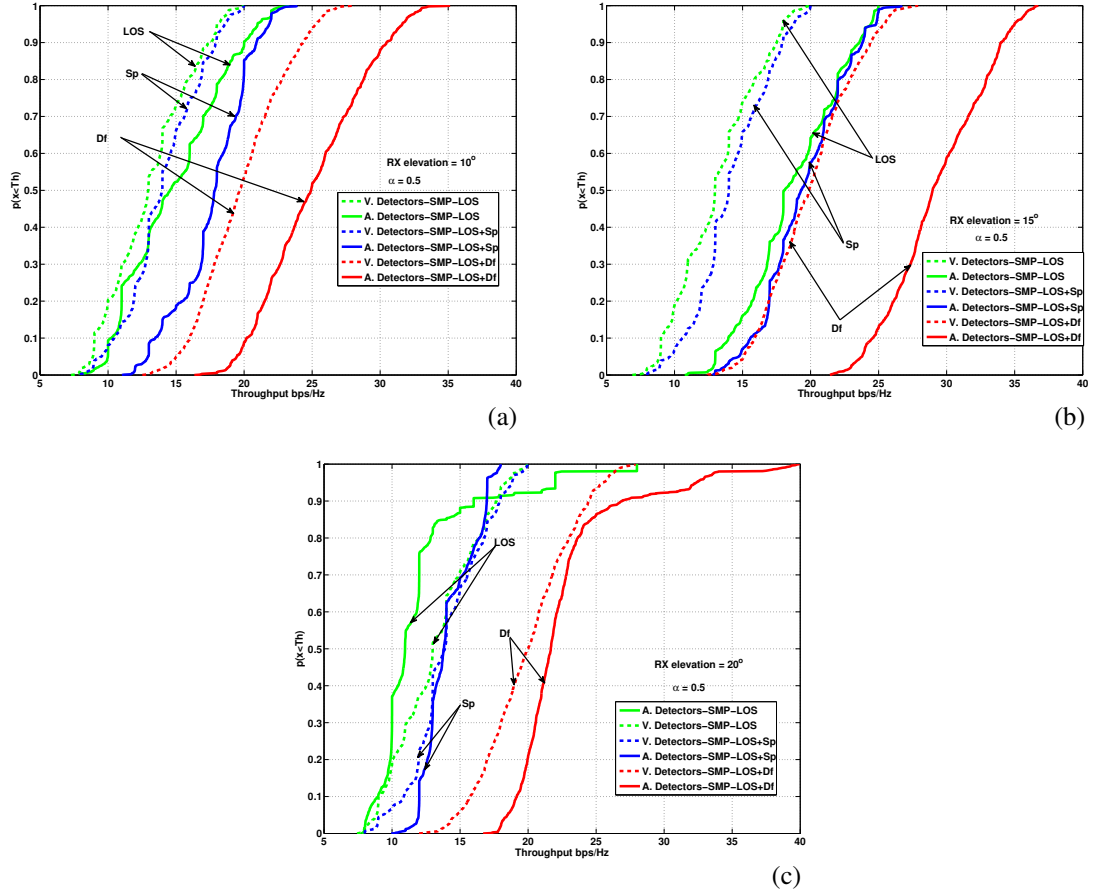
Fig. 5. SMP CDF comparison between three elevation angles in angular diversity receiver detectors when LOS, LOS + Df and LOS + Sp are considered, $\alpha = 0.5$ (a) SMP, 10º (b) SMP, 15º (c) SMP, 20º

have rank 3. Looking at Table III, the RC results show that the average throughput for all specular reflection coefficients does not vary significantly because the same data are transmitted by all transmitting LEDs so whether the rank of channel matrix is 1 or 4, the same data rate is achieved. The specular reflection results in Fig. 6 shows that both detectors setups give non zero throughput because of the gain caused by the specular reflected rays. Also both detector setups have negligible difference in their throughput performance because RC cannot exploit higher MIMO channel rank to increase throughput.

Table III shows the average throughput for SM with specular reflections. It can be seen that SM shows modest improvement even as the specular re flection coefficient (α) increases. It can be seen that the A. detectors setup shows much better (al-

most 100%) performance improvement compared to the V. detectors for the same reflection coefficient ($\alpha = 0.5$). Fig. 7. shows CDF results for SM where we can see that both A. Detector and V. detectors have poor performance due to rank deficient conditions in many locations of the room. This problem is addressed by the ASM approach proposed in this paper.

In Table III the average throughput for ASM improves as the specular reflection coefficient α increases for both two receiver setups. It is shown that the A. detectors has 17% throughput improvement compared to V. detectors for the same reflection coefficient ($\alpha = 0.5$). Fig. 8. shows the CDF results for ASM with three reflection coefficients where we can see that the A. Detector achieves better coverage and hence throughput improvement. The figure

TABLE III. SIMULATION RESULTS FOR LOS WITH SPECULAR REFLECTIONS

| Trans- | Average throughput in bps/Hz | | | | | | | | | | | |
| | V. detectors (0°) | | | | | | A. detectors (15°) | | | | | |
| mission | | | | | | | | | | | | |
Method	LOS	0.1	0.3	0.5	0.7	0.9	LOS	0.1	0.3	0.5	0.7	0.9
RC	6.0	6.0	6.4	7.0	7.1	7.3	6.4	6.9	7.0	7.1	7.2	7.3
SM	1.8	1.8	1.9	2.2	3.8	4.1	2.9	3.1	3.9	4.2	6.3	7.0
ASM	7.5	7.5	8.6	8.8	9.1	9.4	10.0	10.1	10.3	10.3	10.4	10.5
SMP	13.1	13.3	13.7	14.0	14.3	14.6	18.6	18.8	19.1	19.5	20.0	20.4

Legend:
V=Vertically oriented, A=Angular diversity
Parameters **0.1** to **0.9** are the reflection coefficients (α) of the reflecting surface

(a)
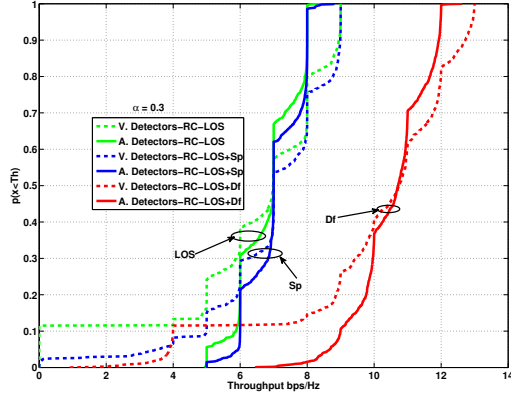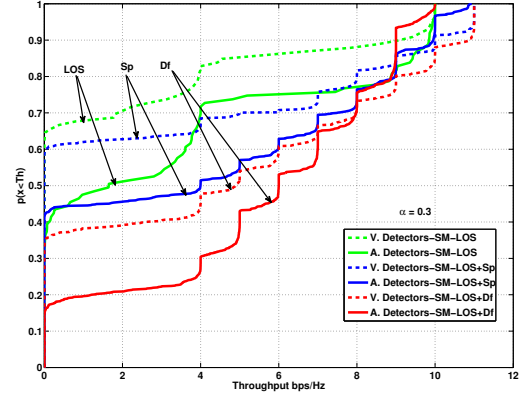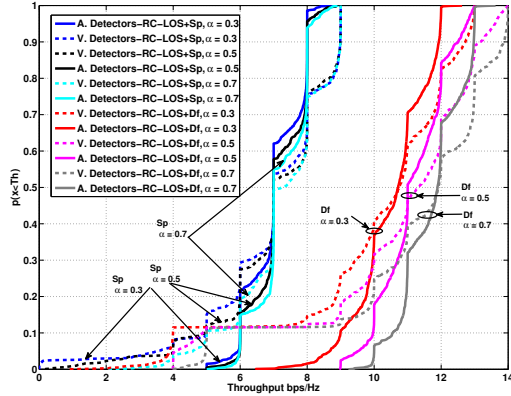
(b)

Fig. 6. RC CDF comparison between three reflection coefficients in vertically and angular diversity receiver detectors when LOS, LOS + Sp and LOS + Df are considered (a) LOS Vs LOS + Sp, $\alpha = 0.3$ (b) LOS + Sp Vs LOS + Df, $\alpha = 0.3, 0.5$ and 0.7.

(a)

(b)

Fig. 7. SM CDF comparison between three reflection coefficients in vertically and angular diversity receiver detectors when LOS, LOS + Sp and LOS + Df are considered (a) LOS Vs LOS + Sp, $\alpha = 0.3$ (b) LOS + Sp Vs LOS + Df, $\alpha = 0.3, 0.5$ and 0.7.

shows that both setups achieve non zero throughput in 100% of the room locations for this propagation environment. Comparing the results of LOS and the effect of specular reflection at $\alpha = 0.5$ we can see that both setups have 100% coverage but there is

22% throughput improvement for A. detectors over V. detectors. Looking at SMP, it shows a significant throughput improvement compared to RC, SM and ASM. This is particularly true because the channel rank for angular diversity detectors is increased to a

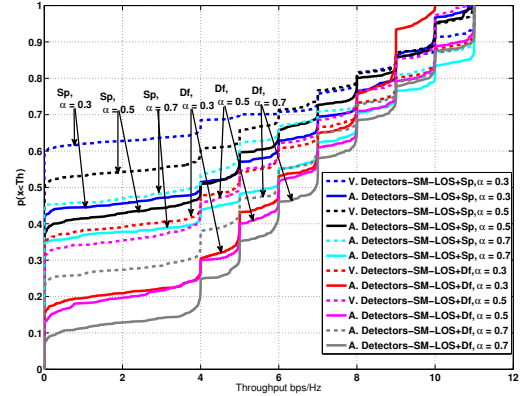higher likelihood of LOS propagation between TX and RX compared to vertically oriented detectors
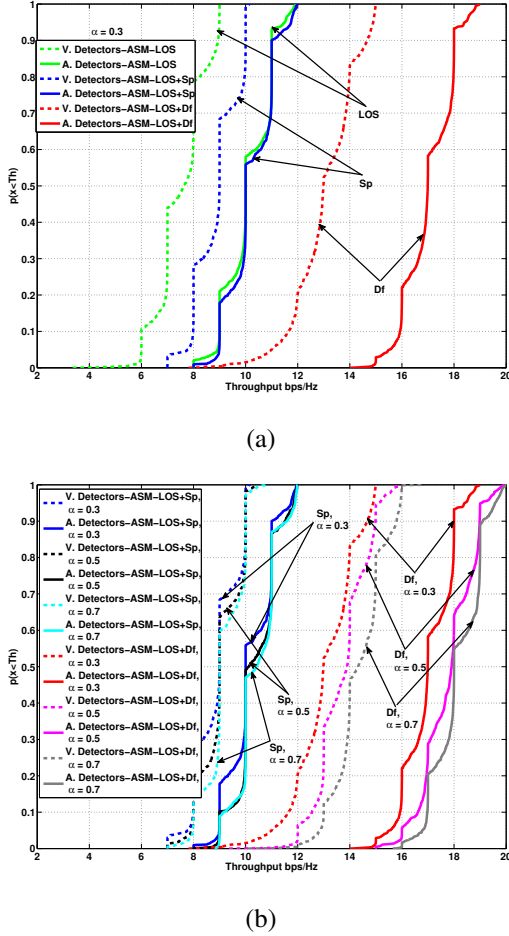

(a)

(b)

Fig. 8. ASM CDF comparison between three reflection coefficients in vertically and angular diversity receiver detectors when LOS, LOS + Sp and LOS + Df are considered (a) LOS Vs LOS + Sp, $\alpha = 0.3$ (b) LOS + Sp Vs LOS + Df, $\alpha = 0.3, 0.5$ and 0.7.

and hence a gain in throughput is observed. Taking reflection coefficient $\alpha = 0.5$ we can see that SMP performs 100% and 175% better than RC for V. Detectors and A. Detectors respectively and when compared to ASM, SMP performs 59% and 89% better for V. Detectors and A. Detectors respectively. We can also notice that increasing α causes a significant improvement in throughput. Fig. 9. also shows that when SMP is used there is a significant difference in throughput between the two setups but that coverage of 100% is achieved for both cases. In the case of specular reflections, the A. detectors shows a 40% improvement compared to

(a)

(b)
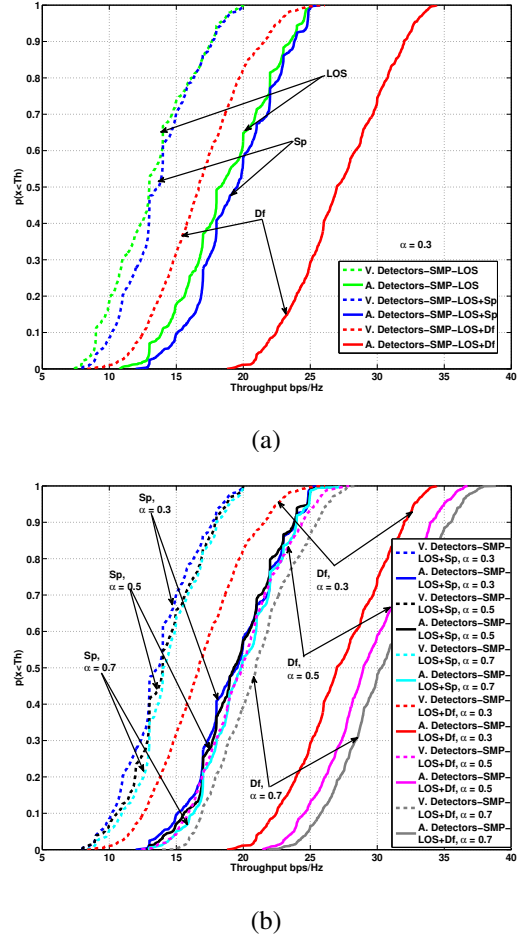
Fig. 9. SMP CDF comparison between three reflection coefficients in vertically and angular diversity receiver detectors when LOS, LOS + Sp and LOS + Df are considered (a) LOS Vs LOS + Sp, $\alpha = 0.3$ (b) LOS + Sp Vs LOS + Df comparison, $\alpha = 0.3, 0.5$ and 0.7.

the V. Detector.

3) Results for LOS with diffuse reflection channel:
Table IV shows simulation results when diffuse reflections are considered. The diffuse reflection case shows a significant effect on system performance. Considering the $\alpha = 0.5$ RC results for the diffuse reflection model shows a $47\text{-}52\%$ improvement compared to those for specular reflection (Table III) in both A. detectors and V. detectors.

Fig. 4 g and h show that when diffuse reflections are considered in both V. detectors and A. detectors, the channel matrix rank is always 4 (100%) for all the reflection coefficients ($\alpha = 0.1$ through 0.9). This is because the diffuse reflection scattered optical channel makes it possible to obtain full MIMO per-

TABLE IV.   SIMULATION RESULTS FOR LOS WITH DIFFUSE REFLECTIONS

Trans-mission Method	Average throughput in bps/Hz											
	V. detectors (0°)						A. detectors (15°)					
	LOS	0.1	0.3	0.5	0.7	0.9	LOS	0.1	0.3	0.5	0.7	0.9
RC	6.0	6.2	9.6	10.4	10.9	11.1	6.4	6.8	10.3	10.8	11.3	11.5
SM	1.8	3.5	4.8	5.1	6.0	6.8	2.9	4.9	6.1	6.4	6.9	7.6
ASM	7.5	7.5	13.2	13.7	14.3	14.6	10.0	14.6	16.9	17.6	18.0	18.4
SMP	13.1	13.1	16.5	19.7	20.8	21.6	18.6	22.4	26.2	29.2	30.4	31.6

Legend:
V=Vertically oriented, A=Angular diversity
Parameters **0.1** to **0.9** are the reflection coefficients (α) of the reflecting surface

formance gains. Looking at the ASM performance in the model including diffuse reflections, we see also a substantial improvement in throughput. Table IV shows that ASM ($\alpha = 0.5$) has 41-56% throughput improvement over the specular reflection results in Table III. For SMP, when diffuse reflections are considered it also shows significant improvement. At $\alpha = 0.3$ in A. detectors, SMP has an improvement of 20-37% over the scenario when only specular reflection is included. In terms of the comparison between V. detector and A. detectors in diffuse reflection conditions with $\alpha = 0.5$, ASM with A. detectors shows 28% throughput improvement over ASM with V. detectors while SMP with A. detectors shows 48% throughput improvement over SMP with V. detectors. Again we can see that, SMP performs 89% and 170% better than RC for V. Detectors and A. Detectors respectively. Generally the diffuse reflection model has shown a big impact on indoor OWC performance due to the of scattered optical power improving the MIMO channel rank statistics.

VI. CONCLUSION

We have presented a mobile angular diversity optical receiver detector model with both specular and diffuse reflections in an indoor visible light communications system. We applied two different reflection models and used a range of reflection coefficients to model different types of reflecting surfaces. We applied different MIMO transmission techniques with adaptive modulation and Per Antenna Rate Control to evaluate the throughput across different room locations. We have compared results for vertical detectors and angular diversity detectors

setups in different scenarios. Our initial results show that using angular diversity detectors increase the likelihood of LOS among transmitters and receivers. It is also shown that in rooms with reflection coefficients of 0.5 or above, diffuse reflection scenarios yield a 50% gain or in system throughput compared to LOS case. For the specular reflection case the gains in throughput are more modest at around 5-10% for reflection coefficients of 0.5 or above.

It is shown that for same setup SMP has better performance compared to other candidates (RC, and ASM). Percentage wise, for specular reflections SMP performs 100% and 175% better than RC for V. detectors and A. detectors respectively while in diffuse reflection SMP performs 89% and 170% better than RC for V. detectors and A. detectors respectively. Compared to ASM, in specular reflections SMP performs 60% and 90% better for V. detectors and A. detectors respectively while in in specular reflections SMP performs 43% and 66% better for V. detectors and A. detectors respectively. It was also seen that, using ASM where we switch between different TX/RX setups, transmission techniques and modulation, we could achieve throughput improvements compared to always using SM with 4 transmitters.

Looking at both LOS, LOS + Sp, and LOS + Df results we can see that ASM performs much better than SM due to its robustness to rank deficient channels. In LOS, ASM performs 317% better than SM with V. detectors and 245% better than SM with A. detectors. In the specular reflection case when we consider $\alpha = 0.5$, ASM performs 300% better than SM with V. detectors and 145% better than SM in A. detectors. Also in the diffuse

refection case when considering the same reflection coefficient, ASM performs 168 % better than SM in V. detector and 175% better than SM in A. detectors. Generally our simulations suggest that, for mobile optical receivers angular diversity detectors can perform better than vertical oriented receivers. When specular or diffuse reflections are included the system performance improves significantly. We have seen the positive impact of reflected optical paths on conditions for the scenarios discussed in this paper. This is because, in the diffuse channels model, receivers can exploit both LOS paths and reflected paths.

REFERENCES

[1] R. Mesleh and H. Haas, "Indoor Optical Wireless Communications; Potential and state-of-art" *IEEE Communication magazine* , Vol. 49, pp. 56-62, September. 2011.

[2] L. Zeng et al. "High data rate multiple input multiple output (MIMO) optical wireless communications using white led lighting", *IEEE Journal in selected Areas in Communications*, Vol 27, pp 1654-1662, December. 2009.

[3] Y. Tanaka et al. "Indoor Visible Light Data Transmission system utilizing White LED lights", *IEICE Transaction on communications*, Vol 8. pp. 2440-2454. Aug. 2003.

[4] D. De-qian and K. Xi-zheng, "A new indoor VLC channel model based on reflection" *Springer optoelectronics letters*, Vol 6, no 4. pp. 295-298, July. 2010.

[5] J. Armstrong, B. Schmidt, "Comparison of asymmetrically clipped optical OFDM and DC-biased Optical OFDM in AWGN", *IEEE Communication letters*, Vol. 12, pp. 343-345, May. 2008.

[6] P. Fahamuel, J. Thompson and H. Haas, "Study, analysis and application of optical OFDM, single carrier (SC) and MIMO in intensity modulation direct detection (IM/DD)" *IET Intelligent Signal Processing Conference 2013*, London, pp. 1-6, December. 2013.

[7] K. Dambul, D. O'Brien, and G. Faulkner, "Indoor Optical Wireless MIMO System With an Imaging Receiver" *IEEE Photonics Technology Letters*, Vol. 23, no.2, pp. 97-99, January. 2011.

[8] D. O'Brien, "Multi-input multi-output (MIMO) indoor optical wireless communications" *Conference Record of the Forty-Third Asilomar Conference on Signals, Systems and Computers* , Pacific Grove, CA, pp. 1636-1639, November. 2009.

[9] L. Tang and W. Chang, "Design of an Omnidirectional Multibeam Transmitter for High-Speed Indoor Wireless Communications" *EURASIP Journal on Wireless Communications and Networking 2010*, Vol 2010, no 65, pp. 1687-1499, April. 2010.

[10] J. Kahn and J. Barry, "Wireless Infrared Communications" *IEEE Proceedings*, Vol 85. no 2, pp. 265 - 298, August. 1997.

[11] R. Mesleh et al, "Indoor MIMO Optical Wireless Communication Using Spatial Modulation" *IEEE International Conference on Communications (ICC)* , Cape Town, South Africa. pp. 1-5, May. 2010.

[12] T. Fath, J. Klaue and H. Haas "Coded Spatial Modulation applied to Optical Wireless Communications in Indoor Environments" *IEEE Wireless Communications and Networking Conference*, Shanghai, China, pp. 1000-1004, April. 2012.

[13] T. Wang, Y. Sekercioglu, and J. Armstrong, "Analysis of an Optical Wireless Receiver Using a Hemispherical Lens With Application in MIMO Visible Light Communications" *Journal of Lightwave Technology*, Vol 31, no 11. pp.1744-1754, June. 2013.

[14] T. Fath and H. Haas, "Performance Comparison of MIMO Techniques for Optical Wireless Communications in Indoor Environments" *IEEE Transactions on Communications*, Vol 61, no 2. pp. 733-742, February. 2013.

[15] T. Wang, R. Green, and J. Armstrong, "Prism Array-Based Receiver with Application in MIMO Indoor Optical Wireless Communica-

tions" *International Conference on Transparent Optical Networks (ICTON)*, Graz, Australia, pp. 1-4, July. 2014.

[16] Y. Wang and N. Chi, "Demonstration of High-Speed 2×2 Non-Imaging MIMO Nyquist Single Carrier Visible Light Communication With Frequency Domain Equalization" *Journal of Lightwave Technology*, Vol. 32, no. 11, pp. 2087-2093, June. 2014.

[17] P. Fahamuel, J. Thompson and H. Haas, "Improved Indoor VLC MIMO channel capacity using mobile receiver with angular diversity detectors" *IEEE Globe Telecommunications conference (GLOBECOM 2014)*, Austin, TX, USA, December. 2014.

[18] S. Grant et al, "Per Antenna-Rate-Control (PARC) in Frequency selective Fading with SIC-GRAKE Receiver" *IEEE Vehicular Technology Conference*, Vol 7, pp. 26-29, September. 2004.

[19] R. Mesleh et al, "Optical Spatial Modulation" *Journal of Optical Communications and Networking, IEEE/OSA*, vol 3, no 3, pp. 234-244, March 2011.

[20] R. Masleh et al. "Spatial Modulation-A New Low Complexity Spectral Efficiency Enhancing Technique" *First International Conference on Communications and Networking in China, 2006. ChinaCom '06*, Beijing, pp. 1-5, October, 2006.

[21] E. Basar et al, "Space-time block coded spatial modulation" *IEEE Transactions on Communications*, Vol 59, no 3, pp. 823-832, March. 2011.

[22] A. Molisch. and M. Win, "MIMO systems with antenna selection" *IEEE Microwave Magazine*, vol 5. no 1, pp. 46-56, March. 2004.

[23] S. Sanayei and A. Nosratinia, "Antenna selection in MIMO systems" *IEEE Communications Magazine*, vol 42. no 10, pp. 68-73, October. 2004.

[24] Y. Ping et al, "Adaptive Spatial Modulation for wireless MIMO transmission systems" *IEEE Communication Letters*,vol. 15. no 6, pp. 602-604, June. 2011.

[25] R. Hari et al, "Antenna selection in spatial modulation systems" *IEEE Communications Letters*, vol.17, no 3, pp. 521-524, March. 2013.

[26] Y. Xiao et al, Power scaling for spatial modulation with limited feedback *International Journal of Antennas and Propagation*,vol. 2013, May. 2013.

[27] P. Yang et al, "Link adaptation for spatial modulation with limited feedback" *IEEE Trans. Vehicular Technology*, vol. 61, no. 8, pp. 3808-3813, October. 2012.

[28] M. Di Renzo et al, "Spatial Modulation for Generalized MIMO: Challenges, Opportunities, and Implementation" *Proceedings of the IEEE*, vol. 102, no 1, pp. 56-103, January. 2014.

[29] M. Di Renzo and H. Haas, " Bit Error Probability of SM-MIMO Over Generalized Fading Channels", *IEEE Trans. Vehicular Technology*, vol. 61, no 3, pp. 1124-1144, January. 2012.

[30] M. Di Renzo and H. Haas, "On Transmit Diversity for Spatial Modulation MIMO: Impact of Spatial Constellation Diagram and Shaping Filters at the Transmitter", *IEEE Trans. Vehicular Technology*, vol. 62. no 9, pp. 2507-2531, February. 2013.

Additional Material: Performance analysis of indoor diffuse VLC MIMO channels using Angular Diversity Detectors

During the review of this paper, one of the reviewers asked the question below. We are providing a copy of the question and our response to assist anyone who is interested in the results reported in this manuscript.

Qu: In particular, Fig. 4(g) of this paper shows that the channel matrix has a full rank, when using Vertical detectors (V. detectors) in all simulation locations. Is this so also in the corner of the room? It might be beneficial to provide more details concerning the channel matrices related to Fig. 4(g) and (h)

Ans: As explained in the paper, the throughput which is affected by the optical channel condition/characteristics which are evaluated at 1000 locations of the room (using 1000 channel matrices). Due to space considerations, it is hard to explain in the paper about all the conditions at each point but some example channel matrices in different scenarios have been extracted from our simulations and are listed below. We hope that this information will assist the reviewer. If the paper is accepted, we will upload this information to the University of Edinburgh data respository, so that readers of the paper can also access this data.

In all the cases considered below we used reflection coefficient = 0.5 the same as the one used in simulations resulted to figure 4(e through h).

CASE 1: For Line of Sight (LOS) channel alone
    a) **Angular diversity detector 15deg from vertical**

Point close to the center (2.7583, 2.7392, 0)

H=
  1.0e-005 *

0.7323	0.3465	0.8582	0.3894
0.7323	0.3465	0.8582	0.3894
0.7323	0.3465	0.8582	0.3894
0.7323	0.3465	0.8582	0.3894

Point at the corner (3.8447, 3.7904, 0)

H=
1.0e-005 *

0.3238	0	0	0
0.3238	0	0	0
0.3238	0	0	0
0.3238	0	0	0

    b) **Vertical detector**

Point close to the center (2.75832, 2.71321, 0)

H=
  1.0e-005 *

  0.6411   0.3172   0.8745   0.3994
  0.6411   0.3172   0.8745   0.3994
  0.6411   0.3172   0.8745   0.3994
  0.6411   0.3172   0.8745   0.3994

Point close to the corner (3.8997, 3.8964, 0)

H =
  1.0e-005 *

  0.4784   0   0.3939   0
  0.4784   0   0.3939   0
  0.4784   0   0.3939   0
  0.4784   0   0.3939   0

COMMENTS ON CASE 1: It can be seen that all of these channels are rank 1, as all the rows of H are identical. In the corner scenario, the vertical detector actually achieves a slightly higher amplitude channel.

CASE 2: For specular reflection plus LOS

a) Angular diversity detector 15deg from vertical

Point close to the center (2.75832, 2.71321, 0)

H =
  1.0e-005 *

  0.8422   0.6797   0.5014   0.4392
  0.6770   0.0208   0.3764   0.0255
  0.0938   0.0623   0.0661   0.0476
  0.0825   0   0.0588   0

Point close to the corner (3.5987, 3.7854 , 0)

H =
  1.0e-005 *

  0.4150   0.2228   0.5976   0.2937
    0   0   0.0064   0.0093
  0.5706   0.3126   0.5932   0.2943
  0.0007   0.0034   0.0066   0.0095

b) Vertical detector

Point close to the center (2.11187, 2.4712, 0)

H =
  1.0e-005 *

  0.4045   0.5056   0.2428   0.2976

```
0.4035   0.3730   0.2455   0.1947
0.1795   0.1541   0.1204   0.1053
0.2116   0.1430   0.1394   0.0985
```

Point close to the corner (3.6887   3.7684 , 0)

H =
 1.0e-005 *
```
0.2199   0.2839   0.1768   0.2091
0.1809   0.2617   0.1456   0.1812
   0        0        0        0
0.1881   0.2271   0.1445   0.1616
```

COMMENTS ON CASE 2: Close to the center, both detectors achieve full rank channel matrices. In the corner location, the angular detector achieves a higher gain channel which is full rank, while the vertical detector experiences a rank 3 channel condition with lower channel gain. For the vertical detector, it appears that the third receiver sensor moves out of the field of view of all transmitters.

CASE 3: For diffuse reflection plus LOS

   a) Angular diversity detector 15deg from vertical

At the point close to the center (2.1653, 2.5371, 0)

H =
 1.0e-005 *
```
0.3638   0.4964   0.4856   0.0744
0.3992   0.3682   0.6192   0.5900
0.2136   0.1863   0.2169   0.9070
0.2291   0.2937   0.2168   0.2015
```

At the corner (0.3180, 0.0013, 0)

H =
 1.0e-005 *
```
0.0360   0.1192   0.1469   0.0761
0.0213   0.0052   0.0225   0.0625
0.0244   0.0996   0.0393   0.0375
0.0131   0.0157   0.0230   0.0371
```

   b) Vertical detector

At the point close to the center (2.4553, 2.4221, 0)

H =
 1.0e-005 *
```
0.6237   0.5621   0.4932   0.5993
0.5351   0.3812   0.4439   0.3987
0.5564   0.6072   0.5973   0.3351
```

0.3151   0.3531   0.1854   0.2416

Point at the corner (3.9881, 3.6079, 0)

H =
 1.0e-005 *
  0.1107   0.0452   0.0514   0.0946
  0.0319   0.0451   0.0169   0.0385
  0.0710   0.0329   0.0228   0.0326
  0.0109   0.0244   0.0246   0.0385

COMMENTS ON CASE 3: Close to the center, both detectors achieve full rank channel matrices but with lower channel amplitudes than the specular case. In the corner location, both receivers appear to benefit from diffuse reflections and observe a higher channel amplitude than for the specular reflection case.